



# CdS/PVA In-Situ Polymerization Composite Films with Enhanced Structural, Optics, Limiting Effect and Electrical Properties

A. Bouzidi<sup>1,2</sup> · I. S. Yahia<sup>3,4,5</sup> · W. Jilani<sup>1,6</sup> · H. Guermazi<sup>1</sup> · S. AlFaify<sup>3</sup> · H. Algarni<sup>3</sup>

Received: 7 December 2017 / Accepted: 19 March 2018 / Published online: 19 March 2018  
© Springer Science+Business Media, LLC, part of Springer Nature 2018

## Abstract

Cadmium sulfide doped Poly(vinyl alcohol) (CdS/PVA) polymeric films have synthesized by using in-situ polymerization technique and ultrasonic approach at the various molar weight of CdS. Subsequently, CdS/PVA polymeric films have been prepared with the objective of studying the effect of CdS nanoparticles on structural, optical and dielectric properties of PVA matrix films. XRD analysis was used to investigate the structural changes of CdS/PVA polymeric films. XRD study evidently shows a cubic crystal structure for CdS powder with the lattice constants  $a = 5.818 \text{ \AA}$  and the space group F-43m. All polymeric films revealed the appearance of smaller new peaks related to the presence of CdS into PVA matrix. The dependence of optical properties was investigated by using UV–vis spectroscopy. The estimated band gaps energies revealed a redshift that confirms the active region in solar cell devices. The optical limiting effect showed a completely UV–Vis blocking of the synthesized polymeric films at the high molar of CdS contents. Dielectric properties were measured by using high-frequency LCR meter (4200-SCS) and were found to be strongly dependent on frequency and molar of CdS concentration. Dielectric permittivities were strongly influenced by the applied angular frequency and the real parts were decreased with increasing the molar CdS concentration. AC conductivity increased with angular frequency and decreased with increase in molar weight of CdS content. The results revealed that all synthesized materials are potentially suitable for optics technology devices.

**Keywords** CdS/PVA polymeric films · Limiting effect · Optical properties · AC electric conductivity

✉ A. Bouzidi  
abdelfattehbouzidi@yahoo.com

<sup>1</sup> Research Unit, Physics of Insulating and Semi Insulating Materials, Faculty of Sciences, University of Sfax, B.P.1171, 3000 Sfax, Tunisia

<sup>2</sup> Technical and Vocational Training Corporation, Technical College Branch, P.O. Box 10, Ahad Rufidah 61974, Kingdom of Saudi Arabia

<sup>3</sup> Research Center for Advanced Materials Science (RCAMS), King Khalid University, P.O. Box 9004, Abha 61413, Kingdom of Saudi Arabia

<sup>4</sup> Advanced Functional Materials & Optoelectronic Laboratory (AFMOL), Department of Physics, Faculty of Science, King Khalid University, P.O. Box 9004, Abha, Kingdom of Saudi Arabia

<sup>5</sup> Nanoscience Laboratory for Environmental and Bio-Medical Applications (NLEBA), Semiconductor Lab., Department of Physics, Faculty of Education, Ain Shams University, Roxy, Cairo 11757, Egypt

<sup>6</sup> Department of Physics, Faculty of Science Sciences and Arts Dhahran Al Janoub, King Khalid University, P.O. Box: 960, Abha 61421, Kingdom of Saudi Arabia

## 1 Introduction

In recent years, the design of advanced functional materials with control in the micro/nanometer scale like semiconductor nanoparticles reinforced with polymeric matrices have involved extensive interest because their size dependent properties and enormous potential for many devices such as optoelectronic application, nonlinear optics, solar cells, heterogeneous photocatalysis, optical windows switching, and single electron transistors [1]. Polyvinyl alcohol (PVA) is a widespread coating industry polymer. PVA is due to its chemical properties and structure a suitable polymer for biomedical applications. PVA is commonly used as textile fiber coatings or as coatings for pills. However, commercial PVA contains some residual vinyl acetate groups as PVA is made by hydrolysis of polyvinyl acetate in methanol [1]. Therefore, commercial PVA is a copolymer of vinyl alcohol and vinyl acetate. A polymer composite film is a material made by adding nanofiller particles in the polymer matrix to form the homogeneous dispersion. Some electrical and optical

properties of polymeric composite films can be very different compared to the neat polymer. This leads to the possibility of developing materials with desired properties. Researchers have used many diverse types of added particles and control of particle size, such as calcium carbonate [2], glass fibers [3], metal oxide nanoparticles [4], and CNTs [5] to enhance the optical, electrical and structural [6] properties of polymers. Incorporation of inorganic nanoparticles in polymer matrices is interesting attention because the combination of both these materials which proves a simple route to stable and processable materials having properties of both components reinforced in the matrix [5]. Colvin et al. [7] studied the CdSe introduced into polymer matrix composites, which enhanced that the prepared systems make suitable for blue light emitters applications. The II–VI semiconductors (CdS) are widely used as window layers of solar cells. CdS are one of the investigated materials. Recently, various research groups have studied the formation of nanocrystalline CdS thin films in diverse ways like spray pyrolysis, chemical bath deposition, vacuum deposition, pulsed laser deposition, etc. Researchers, [8–10] have synthesized the  $\text{Cd}_{1-x}\text{Zn}_x\text{S}$  thin films using co-evaporation of CdS and ZnS powder and have incorporated Zn in CdS nanoparticles. The dielectric properties of varied materials have investigated by several researchers [11–13]. The PVA atoms have carbon chain backbone with hydroxyl groups (–OH) attached to methane carbons; these (–OH) groups can be a source of hydrogen bonding, and hence help the formation of inorganic nanoparticles inside the PVA material [14, 15]. The design and synthesize new materials, the PVA atoms have a relatively large band gap of the functional organic materials and lower the optical absorption which limits its device as an active layer in organic solar cells [16–19]. The incorporation of nanoparticles into PVA matrix has a profound impact on the structural, optical and electrical behaviors of the polymer matrix [20, 21]. The result of this technology has attracted much attention in view of their potential applications in electrical and optical devices. Ali et al., have prepared the CdS/PVA nanocomposite films with different concentrations of  $\text{Cd}^{2+}$  ions using various  $\gamma$ -ray irradiation [22]. It has established the UV–Vis data show a correlation between the estimated optical band gap energies with either  $\text{Cd}^{2+}:\text{S}^{2-}$  molar ratio.

The polyvinyl alcohol (PVA) is a soluble transparent and highly durable nature has been used as a host matrix for incorporating the molecular cadmium sulfide (CdS) using in-situ ultrasonic polymerization. Several characterization methods have been used to explore the effect of CdS molecular weight loading on the properties of CdS/PVA composite polymeric films in detail. The aim of this study is to characterize the CdS/PVA composite polymeric films with investigating the crystal structure, the optical and dielectric

properties in connections to stand up their advantages in the new designed optoelectronic applications.

## 2 Experimental and Characterization Methods

### 2.1 CdS/PVA Composites Polymeric Films Preparation

All chemicals reagents were used without further purification. The monohydrate cadmium chloride is anhydrous (from look for chemicals industries  $\text{CdCl}_2 \cdot \text{H}_2\text{O}$  molecular weight, 201.32 g/mol. Sodium sulfide  $\text{Na}_2\text{S}$  has a molecular weight 78.04 g/mol (Sigma-Aldrich). The polyvinyl alcohol is a polymer matrix produced by LOBA Company, India. It was used without any purification). Polyvinyl alcohol is a polymer matrix produced by LOBA Company, India. It was used without any purification.

An aqueous solution of pure Polyvinyl alcohol (PVA) matrix was synthesized by dispersing 45 g of powder into 1 L deionized water by using magnetic stirring for 48 h at 80 °C. Finally, we obtained the PVA transparent after lifting the residuals in the bottom of the PVA bottle. Different molar concentrations (0.001, 0.01 and 0.05 M) of cadmium chloride ( $\text{CdCl}_2$ ) as a source of cations ( $\text{Cd}^{2+}$ ) and Sodium sulfide  $\text{Na}_2\text{S}$  as a source of anions ( $\text{S}^{2-}$ ) were separately prepared in the 5 mL distilled water at room temperature.

The CdS/PVA composites polymeric films were prepared and synthesized using in-situ polymerization ultrasonic probes. Firstly, we dissolved in 60 ml PVA with 20 ml CTAB (5 g/L) a molar quantity of  $\text{CdCl}_2$ . Then, the obtained mixture was placed and stirred in a well-equipped ultrasonic probe for a time 5 min. Now, we added a molar content of  $\text{Na}_2\text{S}$  for the obtained mixture. The resulting mixture was transferred to Petri dish and dehydrated in an oven for 3 days at fixed temperature around 40 °C. Finally, the dried formed composite polymeric films were studied for further characterization.

### 2.2 Devices and Measurements

The prepared CdS/PVA composites polymeric films have tested using a Shimadzu Lab XRD-6000 diffractometer of monochromatic *CuK $\alpha$*  radiation substance performed at the 40 kV of voltage and a 30 mA of current of with an increment of 0.02°/s in the angular range of 5°–90° for confirming the crystallography structure of the tested sample.

The transmittance  $T(\lambda)$ , absorbance  $A(\lambda)$  and reflectance  $R(\lambda)$  of CdS/PVA polymeric composite films were measured by using JASCO V-570 spectrophotometer in the wavelength number from 190 to 2500 nm at the room temperature for the

normal light incidence. The various optical parameters were calculated based on the above measurements.

The Optical limiting effect recorded for the CdS/PVA composite polymeric films by using a He–Ne laser of 632.8 nm. The focal lens of 10 cm was fixed on an optical bench. After that polymeric film sample holder adjusted to be the focal point of the lens. Input /output powers of the applied He–Ne laser were measured by using optical laser power meter attached with photo-detector (Model: Newport 1916-R). Then, the designed holder was suitable for polymeric films.

For measuring AC-electrical conductivity at room temperature, the CdS/PVA polymeric films were placed among binary Cu-brass holder using a unique designed holder. Semiconductor characterization system from Keithley was used to measure the AC/dielectric parameters as follows: the impedance  $Z$ , the capacitance  $C$ , and the loss factor ( $\tan\delta$ ) in connections as installed inside the device software.

For the investigated samples, the AC electrical conductivity  $\sigma_{AC}$  of CdS/PVA composite polymeric films were analyzed at room temperature over a wide scale of frequency from 3 kHz to 10 MHz. It was obtained according to the following equations [23, 24]:

$$\sigma_{Total.AC} = \frac{d}{ZS}, \quad (1)$$

$$\sigma_{Total.AC} = \sigma_{AC} + \sigma_{DC}(\omega \rightarrow 0), \quad (2)$$

$$\sigma_{AC} = B\omega^s, \quad (3)$$

where  $\sigma_{Total.AC}$  is the total electrical conductivity,  $B$  is a constant,  $\omega$  is the angular frequency and  $s$  is the frequency exponent parameter. Dielectric permittivity  $\epsilon'$  was determined using the expression [25]:

$$\epsilon' = \frac{Cd}{\epsilon_0 S} \quad (4)$$

where  $C$  stays the measured capacitance of the sample,  $\epsilon_0$  is the free space permittivity and  $d$  is the sample thickness of the films,  $S$  represents is the effective area.

The imaginary part dielectric factor loss  $\epsilon''$  was evaluated by the following equation [25]:

$$\epsilon'' = \tan \delta \times \epsilon' \quad (5)$$

where  $\tan \delta$  is the obtained measured loss tangent.

## 3 Results and Discussions

### 3.1 Crystal Structure Analysis

After the preparation of the CdS/PVA polymeric films, they were characterized by XRD analysis. The XRD

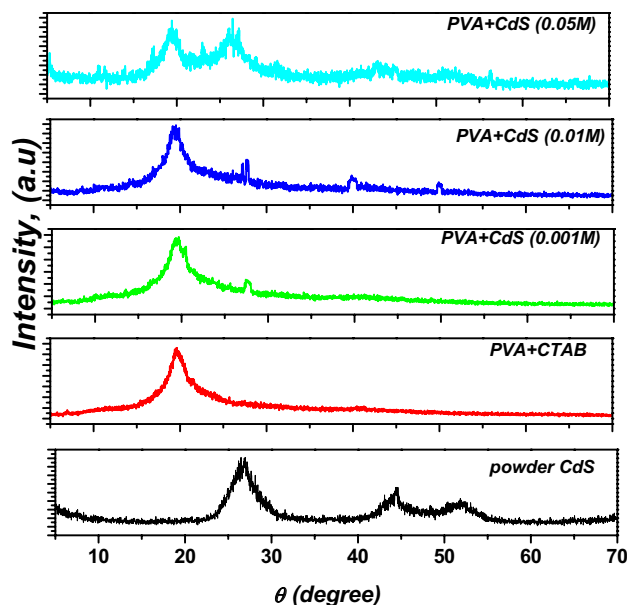


Fig. 1 XRD pattern characterization of CdS/PVA in situ polymeric films

patterns of CdS nanoparticles and their CdS/PVA composites polymeric films were presented in Fig. 1. As shown in Fig. 1, it is clearly revealed the formation of single phase CdS with a cubic crystal structure with the standard (ICDD card No. 01-080-0019) [26], the space group  $F-43m$  (216) and with a cell parameter ( $a = 5.818 \text{ \AA}$ ). Typical peaks at  $2\theta = 26.94^\circ$ ,  $44.43^\circ$  and  $52.01^\circ$  assigned to (111), (220), and (311) planes can be used to analyze the alignment orientation of CdS nanopowders.

The XRD profiles of the PVA/CTAB and CdS/PVA in situ polymeric composite films with 0.001, 0.01, and 0.05 M (molar) of CdS respectively are shown in Fig. 1. For the prepared PVA/CTAB polymeric film, it is noted the presence of amorphous and crystalline peaks around  $2\theta = 20^\circ$ , which explained the semi-crystalline nature of PVA matrix. The semi-crystalline nature of PVA results from the strong intermolecular interaction between PVA matrix networks. This behavior has also reported by several types of research [27]. The represented XRD patterns of CdS/PVA polymeric films revealed a peak at approximately  $2\theta = 19.4^\circ$ , which confirmed the result obtained by Bhadra et al. [28]. All polymeric films showed the appearance of smaller new peaks at 27.2, 27.88, 39.64 and 49.82, respectively which related to the presence of CdS grafting inside the PVA matrix. Presence of smaller peaks in the XRD pattern confirms that CdS/PVA polymeric composite films are crystalline in nature. Therefore, the main characteristics of CdS/PVA polymeric films are characterized using the optical UV–Vis–NIR spectroscopy.

### 3.2 Optical UV–Vis–NIR Spectroscopy Analysis

The transmittance and absorbance curves for several smart optical CdS/PVA polymeric films in the wavelengths region of 190–2500 nm are shown in Fig. 2a, b, respectively. As shown in this Fig. 2a, a high optical transparency of about 80% is observed for pure PVA in the UV–Vis region. The CdS/PVA polymeric composite films showed an optical transparency vary from 80 to 20% in the visible and IR regions for different molar of CdS particles. At the shorter wavelengths, it is noted decreases in the transmission of the incident light for different CdS/PVA composites films, which may be explained to the layer formed by intermolecular hydrogen interaction bonding between the pure PVA matrix chains and the molar CdS. The prepared polymeric films are being evidenced for stronger absorption of UV–Vis light region (Fig. 2b) and begin a completely blocking light in the range between 190 and 500 nm for the 0.05 M CdS sample. This behavior can make the obtained system suitable used for smart scale polymeric ultrathin films and smart sensors for large-scale optoelectronic applications. A similar result is an agreement with other works [27, 29]. The absorbance

spectrum of pure PVA is lower than the CdS/PVA polymeric films. The absorbance curves of CdS/PVA polymeric films have higher absorption in the wavelengths range from 190 to 500 nm. In the UV–Vis region, it can be provided to produce the smart optical laser blocking filters. As increasing the CdS contents into PVA matrix, the absorption spectra are shifted to a higher UV–Vis wavelength region, which explained by the interaction and the high immersing of CdS molecules inside the PVA during the in-situ polymerization process. These results revealed that the synthesized materials are suitable for optics technology applications. Using the measured absorbance data, the absorption coefficient ( $\alpha$ ) attributed to the absorption edge was calculated in the fundamental absorption region using Lambert's law [30, 31]:

$$\alpha = \frac{2.303 \times A}{t}, \quad (6)$$

where  $A$  is the optical absorbance and  $t$  is the composite films thickness.

Using Tauc's model, the optical constant band gap  $E_g$  was characterized for modeling and explicate the optoelectronic behaviors of the synthesized polymeric films. It was calculated by the following expression [32–34]:

$$(ah\nu)^m = A(h\nu - E_g), \quad (7)$$

where  $A$  is the pre-factor constant which independent of photon energy for this transition, in this case,  $m=2$  and  $m=1/2$  are a parameter describes the nature of the optical transition assuming that the band transition is direct and indirect allowed transition, respectively.

Figure 3a shows the variation of  $(ah\nu)^2$  plots and the photon energy ( $h\nu$ ) for pure PVA film and CdS/PVA polymeric films. The band gap energies were obtained by using the linear portions fitting of the graph to the  $x$ -axis at  $(ah\nu)^2=0$  and were gathered in Table 1. Figure 3b shows the  $(ah\nu)^{1/2}$  plots versus  $(h\nu)$  of indirectly allowed transitions for different polymeric films. The obtained indirectly band gaps were added in Table 1. The analysis of the optical band gaps of these composite polymeric films was closed to indirectly allowed transition band gaps. As shown in Table 1, all band gaps energies decrease with increasing the molar concentrations of CdS compared to PVA matrix and PVA + CTAB film. It shows a redshift as increasing the incident photon energy ( $h\nu$ ). However, the immersing CdS molar concentrations in PVA matrix lead to decrease the energy band gaps which provide the active region in the solar cell of polymeric composite films. This change could be explained by means of the band gap engineering (varying from 5.451 to 2.163 eV for direct band gap) for PVA via the interaction between the molar concentrations of CdS and their PVA molecular chains. Related results are agreeing with that reported by Yahia et al. for Cong red dye doped PVA films [27]. The band gaps enhanced the light absorption of polymeric

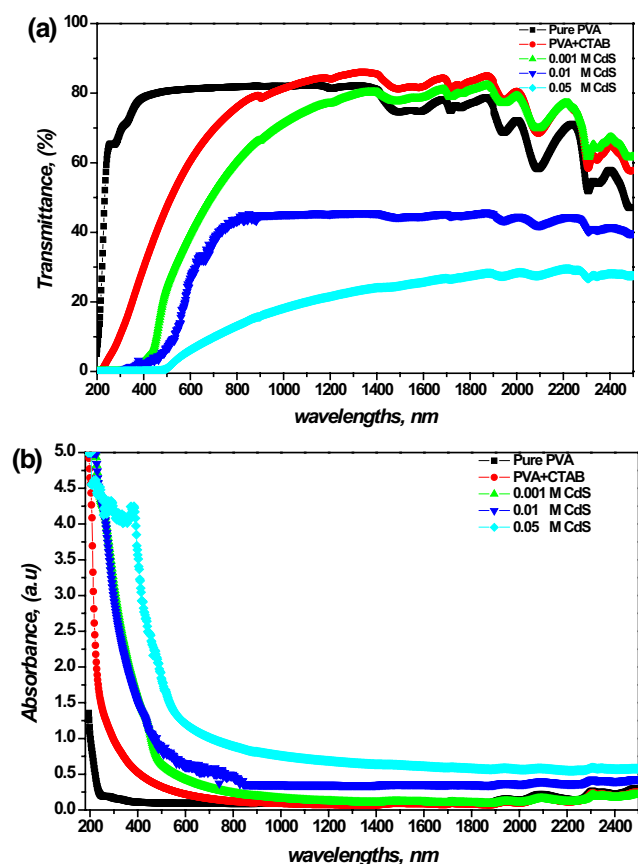


**Fig. 2** **a** Transmittance curves for several smart optical CdS/PVA polymeric films in the wavelengths region of 190–2500 nm. **b** Absorbance data for several smart optical CdS/PVA polymeric films

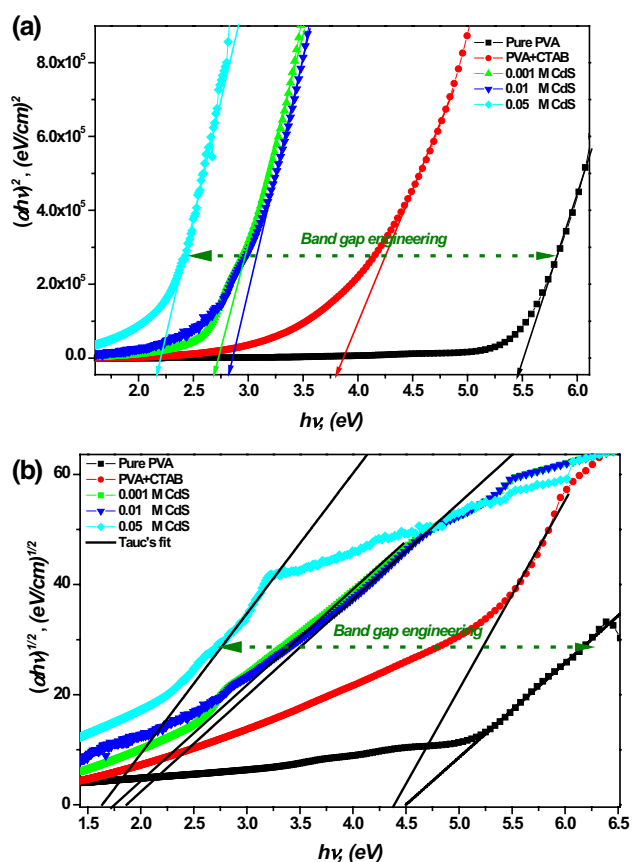


**Fig. 3** a  $(\alpha hv)^2$  plots and the photon energy ( $h\nu$ ) for pure PVA film and CdS/PVA polymeric films (the solid line represents the Tauc's fitting data). b  $(\alpha hv)^{1/2}$  plots versus  $(h\nu)$  of indirectly allowed transitions for different polymeric films (the solid line represents the Tauc's fitting data)

composite films which can be used in optical technology applications. Existing polymeric films are suggested to be used for the fabrication of optoelectronic devices.

### 3.3 Limiting Effect Characterization of CdS/PVA Polymeric Films

To carry out the normalized power measurements using the conventional Z-scan system, the sample holder is scanned across the medium focus of the z-axis producing the open aperture Z-scan. The characteristic of the aperture Z-scan can afford the magnitude of the nonlinear power. It is very interesting applied method to characterize the composite films which have a low transmittance at high molar content.

The optical limiting effect arises from the Z-scan response for the synthesized polymeric films were shown in Fig. 4. At wavelength 638.2 nm laser pulse, the CdS/PVA polymeric films displayed an exponential variation in normalized power with increasing the molar weight of CdS. The normalized power of the obtained composite films would decrease with increasing power intensity. This result provides the completely UV–Vis blocking of the synthesized polymeric films at high molar content of CdS and make these materials suitable for optical laser filters.

### 3.4 Electrical Bulk Conductivity Behaviors of CdS/PVA Films

The AC characteristic response of the samples was investigated to identify the origin of the conduction process and gives information about the behavior of electric charge carriers and on the electrical properties of polymeric films and their interface with electronically conducting electrodes. The dielectric response of polymeric films was studied at room temperature in the frequency range 3 kHz–10 MHz. The real and imaginary dielectric permittivity parts  $\epsilon'$  and  $\epsilon''$  are plotted in Fig. 5a, b. It is observed from this figure that the values of  $\epsilon'$  and  $\epsilon''$  were strongly influenced by the angular frequency. First, the real parts of the dielectric permittivity decrease as increasing the molar concentrations of CdS (Fig. 5a). It showed some increases in their values at lower frequencies which explained by electrode effects become dominant over most of the frequency range at room temperature. At low frequencies, the  $\epsilon'$  exhibits very strong dispersion. This event is attributed to the low frequency space charge accumulation effect. At high frequencies, the  $\epsilon'$  decrease and show a plateau as due to dipole motions. This can be explained by the fact that as the frequency increased, the interfacial dipoles had less time to orient themselves in the direction of the alternating field. The plateau seen in the real part of the dielectric permittivity is due to dipole polarization. Though we expect the plateau at high frequencies, there is also a weak plateau at lower frequencies in the room temperature data, indicating the presence of a relaxation processes at different frequencies. From Fig. 5a, the  $\epsilon'$  value gradually decreased with increase in CdS loading from PVA/CTAB to 0.001 M CdS film compared to the PVA matrix. Also, less difference was observed between  $\epsilon'$  values for PVA/CTAB and 0.001 M CdS films as compared to the  $\epsilon'$  values for 0.01 and 0.05 M CdS. These results suggest that there is existing threshold

**Table 1** Optical parameters like directly and indirectly band gaps transition for pure PVA and CdS/PVA polymeric films

Samples		Pure PVA	PVA + CTAB	0.001 M CdS	0.01 M CdS	0.05 M CdS
Direct band Gap	$E_g^{(d)}$ (eV)	5.451	3.802	2.823	2.685	2.163
Indirectly band Gap	$E_g^{(i)}$ (eV)	4.494	4.375	1.855	1.739	1.628

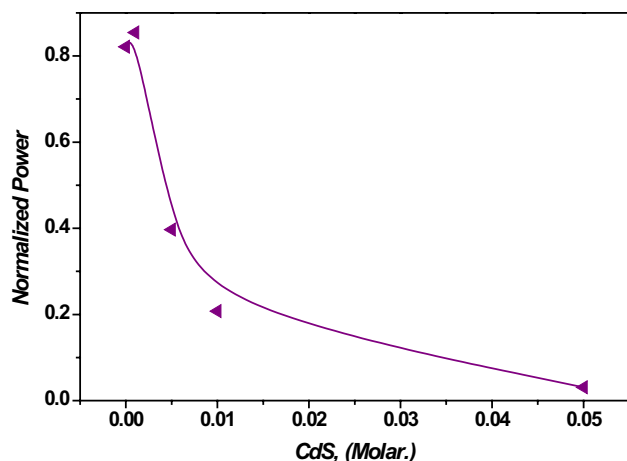


**Fig. 4** Optical limiting effect arises from the Z-scan response for the synthesized polymeric films

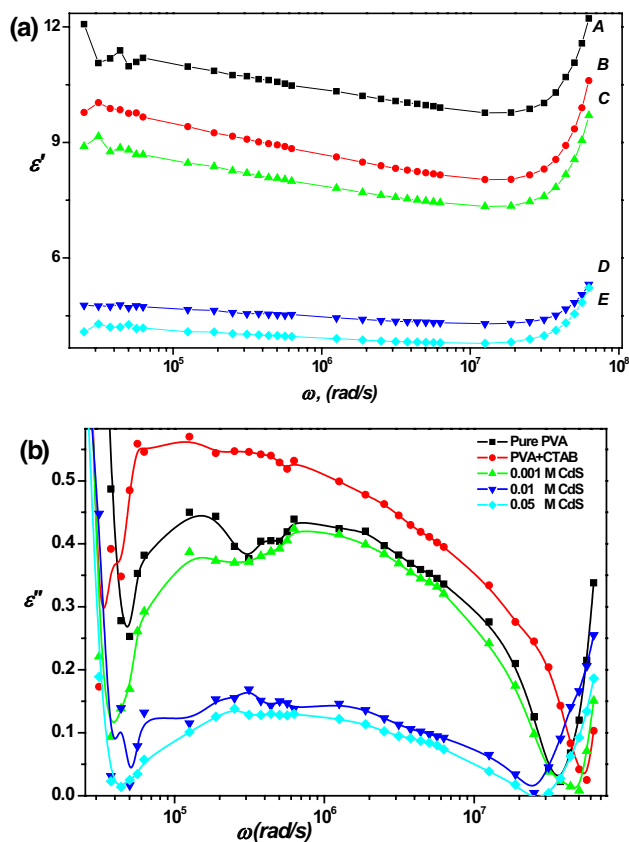


**Fig. 5** **a** The real plots of the dielectric permittivity parts  $\epsilon'$  for CdS/PVA polymeric films (A pure PVA, B PVA + CTAB, C 0.001 M CdS, D 0.01 M CdS and E 0.05 M CdS). **b** The imaginary plots of the dielectric permittivity parts  $\epsilon''$  for polymeric films

CdS molar concentration for the dielectric behavior of these polymeric composite films. Figure 5b represents the imaginary part of the dielectric permittivity as function of frequency. It is seen that the imaginary parts of the dielectric

permittivity  $\epsilon''$  decrease when the frequency goes down. The value of  $\epsilon''$  increased with increasing frequency, which can be credited to the high interfacial traps formed at the CdS/PVA interface that negatively influences the electrical properties. This increase is substantial at high frequencies in the range of  $10^5$ – $10^6$  rad/s and may be due to heat generated within the composite because of rapid alignment of dipoles with the rapidly changing direction of electric field. The imaginary parts of the dielectric permittivity  $\epsilon''$  may have also increased because of increase in conduction losses with increase in frequency. This result can be explained the considering time available for the molecular dipoles to follow the field. The appearance of several peaks in the graph (Fig. 5b) imply that there is more than one relaxation process in CdS/PVA in situ polymerization films, that because they are dominated by the DC conduction mechanism and they are becoming very high due to free charge motion within the material and are connected to AC electrical conductivity relaxation [35].

The dependence of AC electrical conductivity of angular frequency at room temperature for CdS/PVA in situ polymerization films is illustrated in Fig. 6a. It can be noted that the AC electrical conductivity generally increased with increasing the angular frequency, especially at high frequencies. This increment in AC conductivity attributed to the hopping mechanism that occurs under the influence of an externally applied electrical field which may be due to increasing the electronic interaction processes inside the polymeric films because of which the films become more relatively conductive and the polymer chains become more flexible. The AC electrical conductivity  $\sigma_{ac}$  has dispersed to all frequencies regions. It was analyzed using the Jonscher's relation power law. Here, the Jonscher's fitting power law parameters for the synthesized CdS/PVA in situ polymerization were obtained and illustrated in Fig. 6b, c.

The exponent  $S$  of the CdS/PVA polymeric films comprises  $0 \leq S \leq 1$  (Fig. 6b). It has been associated with the presence of defects or impurities, charge carriers and extrinsic dipoles motions. The values of DC electric conductivity are decreased in CdS/PVA polymeric films with different molar of CdS particles compared to pure PVA (Fig. 6c). The change in DC electric conductivity can prove the relatively conductive behavior of these films. The need frequencies on the AC electrical conductivity related to the charge hopping carriers of small range with the trap sites separated by energy barriers of different heights [36, 37].

## 4 Conclusion

In the present work, we have used an XRD, UV–Vis and Dielectric spectrometers to study the effect of the molar weight of CdS on the structural, optical and dielectric

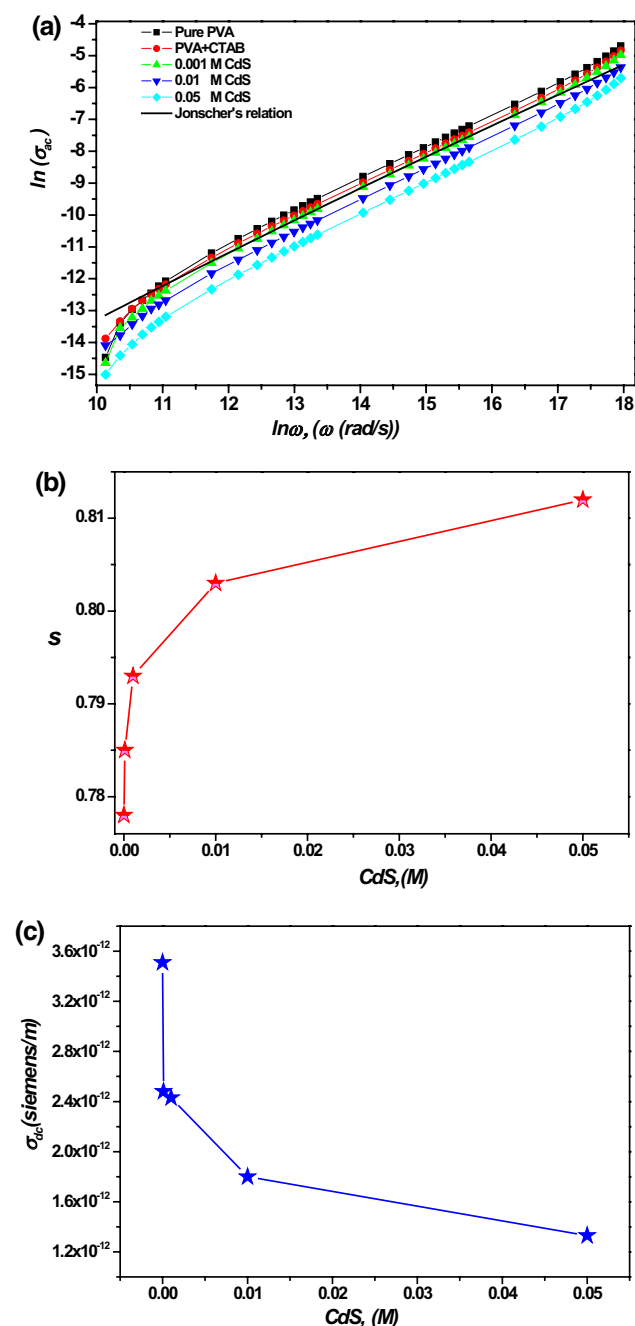


**Fig. 6** a The AC electrical conductivity versus angular frequency for CdS/PVA polymeric films (the solid line represents the Jonscher's fitting data). b Variation of exponent  $S$  versus molar weight of CdS for the CdS/PVA polymeric films. c Variation of the DC electric conductivity for CdS/PVA polymeric films with different molar of CdS

properties for CdS/PVA in situ polymeric films. The XRD analysis indicated that the PVA + CTAB film exhibited a typical amorphous and semi-crystalline structure. The prepared CdS/PVA in situ polymeric films are being evidenced for stronger absorption of UV–Vis light region and begin a completely blocking light in the range between 190 and

500 nm for the 0.05 M CdS sample, which becomes used for smart scale polymeric ultrathin films and smart sensors for large-scale optoelectronic applications. The decreases in band gaps transitions enhanced the light absorption and make these materials suitable used in optical technology applications. The optical limiting effect arises from the Z-scan response for the synthesized CdS/PVA in situ polymeric films show a decrease on normalized power, which provide the completely UV–Vis blocking of the high molar content of CdS and make these materials suitable used for optical laser filters. The dielectric permittivity decreased with the increase in the angular frequency and with the increase in adding the molar concentration of CdS. Moreover, the dependence of AC electrical conductivity with applied frequency was analyzed using the Jonscher's fitting law. The investigated properties were observed to be strongly dependent upon the applied of angular frequency and the molar content of CdS. These characteristics of CdS/PVA polymeric films believed that the hopping of charge carrier motions mechanism associated to the presence of defects or impurities, charge carriers and extrinsic dipoles motions which provide the relatively conductive behavior.

**Acknowledgements** The authors express their appreciation to the Deanship of Scientific Research at King Khalid University for funding this work through research groups program under Grant Number R.G.P.2/9/38.

## References

1. Z. Qiao, Y. Xie, G. Li, Y. Zhu, Z. Qian, *Mater. Sci.* **35**, 285 (2000)
2. R.D.K. Misra, P. Nerikar, K. Bertrand, D. Murphy, *Mater. Sci. Eng.* **384**, 284 (2004)
3. A.T. Di Benedetto, *Mater. Sci. Eng.* **302**, 74 (2001)
4. M. Rubinstein, R.H. Colby, *Polymer Physics*. (Oxford University Press, Oxford, 2003)
5. P. P'otschke, S.M. Dudkin, I. Alig, *Polymer* **44**, 5023 (2003)
6. S.H. Rashmi, A. Raizada, G.M. Madhu, A.A. Kittur, R. Suresh, H.K. Sudhina, *Plast. Macromol. Eng.* **44**, 33 (2015)
7. V. Colvin, M. Schlamp, A.P. Alivisatos, *Nature* **370**, 354 (1994)
8. P.D. Persans, L.B. Lurio, J. Pant, G.D. Lian, T.M. Hayes, *Phys. Rev. B* **63**, 115320 (2001)
9. J.P. Enriquez, X. Mathew, *Sol. Energy Mater. Sol. Cells* **76**, 313 (2003)
10. H. Oumous, H. Hadiri, *Thin Solid Films* **386**, 87 (2001)
11. V. Krishanji, S. Kalyane, *Glob. Res. Anal.* **2**, 225 (2013)
12. S. Suresh, *Appl. Nanosci.* **4**, 325 (2014)
13. R.R. Deshmukh, G.A. Arolkar, S.S. Parab, *Int. J. Chem. Phys. Sci.* **1**, 40 (2012)
14. S.F. Bdewi, O.Gh. Abdullah, B.K. Aziz, A.A.R. Mutar, *J. Inorg. Organomet. Polym. Mater.* **26**, 326 (2016)
15. M.H. Makled, E. Sheha, T.S. Shanap, M.K. El-Mansy, *J. Adv. Res.* **4**, 531 (2013)
16. P.M. Buschbaum, *Adv. Mater.* **26**, 7692 (2014)
17. R. Kroon, M. Lenes, J.C. Hummelen, P.W.M. Blom, B.D. Boer, *Polym. Rev.* **48**, 531 (2008)
18. C. Kanimozhi, P. Balraju, G.D. Sharma, S. Patil, *J. Phys. Chem. B* **114**, 3095 (2010)

19. E. Sheha, H. Khoder, T.S. Shanap, M.G. El-Shaarawy, M.K. El-Mansy, *Optik* **123**, 1161 (2012)
20. L.L. Beecroft, C.K. Ober, *Chem. Mater.* **9**, 1302 (1997)
21. R.V. Kumar, R. Elgamiel, Y. Diamant, A. Gedanken, *Langmuir* **17**, 1406 (2001)
22. Z.I. Ali, F.H. Abd Salam, H.H. Saleh, H.A. Youssef, R. Sokary, *Int. J. Chem. Mater. Environ. Res.* **2**, 17 (2015)
23. I.S. Yahia, H.Y. Zahran, F.H. Alamri, *Synth. Met.* **218**, 19 (2016)
24. O. Kaygilia, S. Keserb, T. Atesa, S. Keser, A.A. Al-Ghamdi, F. Yakuphanoglu, *Spectrochim. Acta A* **129**, 268 (2014)
25. A. Tataroglu, S. Altundal, M.M. Bulbul, *Micro-electron. Eng.* **81**, 140 (2005)
26. Y.A. El-Gendy, I.S. Yahia, F. Yakuphanoglu, *Mater. Res. Bull.* **47**, 3397 (2012)
27. I.S. Yahia, M.A.S. Sherif, Keshk, *Opt. Laser Technol.* **90**, 197 (2017)
28. J. Koteswararao, R. Abhishek, S.V. Satyanarayana, G.M. Madhu, V. Venkatesham, *Express Polym. Lett.* **10**, 883 (2016)
29. A. Costela et al., Medical applications of dye lasers, in *Tunable Laser Applications*, 2nd edn., ed. by F.J. Duarte (CRC, New York, 2009)
30. F. Yakuphanoglu, M. Sekerci, E. Evin, *Phys. B* **382**, 21 (2006)
31. K.S. Hemalatha, K. Rukmani, N. Suriyamurthy, B.M. Nagabhushana, *Mater. Res. Bull.* **51**, 438 (2014)
32. P. Tao, A. Viswanath, L.S. Schadler, B.C. Benicewicz, R.W. Siegel, *ACS Appl. Mater. Interfaces* **3**, 3638 (2011)
33. P. Singh, A. Kaushal, D. Kaur, *J. Alloy. Compd.* **471**, 11 (2009)
34. R.M. Ahmed, *Int. J. Photoenergy* **150389**, 7 (2009)
35. F. El-Kabbany, S. Taha, M. Hafez, *Spectrochim Acta* **128**, 481 (2014)
36. H. Kharrat, N. Elfaleh, S. Kamoun, *J. Phys. Org. Chem.* (2016). <https://doi.org/10.1002/poc.3577>
37. B. Roling, A. Happe, K. Funke, M.D. Ingram, *Phys. Rev. Lett.* **78**, 2160 (1997)